THE JOURNAL OF PHYSICAL CHEMISTRY C

Article

pubs.acs.org/JPCC

Effects of Current-Induced Forces on Pt−Benzene−Pt Single-Molecule Junctions

Bailey C. Hsu,[†] Ilias Amanatidis,[†] Wei-Lin Liu,[†] Allen Tseng,[†] and Yu-Chang Chen*[,†]

[†]Department of Electrophysics, National Chiao Tung University, 1001 University Road, Hsinchu 30010, Taiwan

[‡]National Center for Theoretical Sciences, National Chiao Tung University, 1001 University Road, Hsinchu 30010, Taiwan

ABSTRACT: From first-principles approaches, we investigate the torque exerted by the current-induced forces in a highly asymmetric molecular junction, where the benzene molecule is directly connected to the platinum electrodes. We observe that the curved flow of the current streamline around the tilted molecule can induce a net torque, which tends to rotate the benzene molecule, much like the way a stream of water rotates a waterwheel. The magnitude and direction of the net torque are determined by the detailed current density flowing through the molecular junction. Such an asymmetric molecular junction could offer an experimentally practical system for the exploration of an electrically controllable single-molecule motor. The idea given above is also supported by a simple physical model based on the Landauer−Büttiker formula in the tight-binding framework.

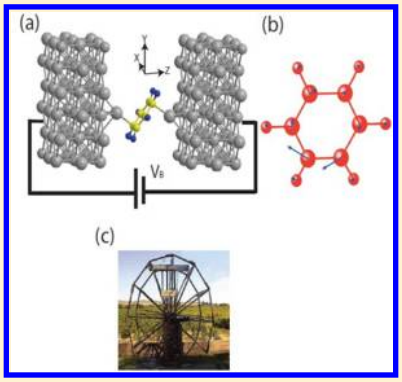

I. INTRODUCTION

In the new emerging field of nanoelectromechanics (NEMS), the controlling operation of nanometer-sized (molecular) devices remains both critical and challenging.[1−3] It is naturally accepted that molecular motors will play an important role in the design of these nanomachines since in the macroscopic world the basic component of any machine is a motor. Several studies have examined molecular motors driven by light, chemical reaction, and current.[4−16] We propose a conceptually new design of an electrically controllable single-molecule motor, propelled by the current-induced forces due to nonequilibrium coherent electron transport. We investigate from first-principles calculations the torque that is exerted by the current-induced forces in an asymmetric single-molecule junction. Current-induced forces arise from the current flowing through the nanojunction. These forces are exerted by scattered electrons via the change of their momentum transferred to the molecule and can be decomposed into two components: the direct force and the wind force. The direct force is the electrostatic force acting on the core electron charge due to the electrostatic field induced by the voltage applied across the junction, whereas the wind force is due to the current-carrying electronic states which cause the net momentum transfer from electrons scattered by the ions.[17] The wind force is proportional to the rate of momentum transfer from the electrons to the ions. In microelectronics, this phenomenon is known as electromigration, which is one of the major mechanisms that frustrate the metallic contacts.[18] The nanojunction may carry much larger current density than the macroscopic counterparts. Consequently, the current-induced forces are of key importance to understand the mechanical instability of the nanojunction.[19] For example, in the case of a single atom in the vacuum between two electrodes with a semi-infinite planar surface, the scattering of electrons at the atom creates a resonant charge dipole centered at the atom in the same direction as the electron flow. This has a current-induced force against the electron flow just like the local resistive dipole in electromigration.[20] Also, we note that the inelastic electron−vibration interactions contribute negligibly to current-induced forces in quasi-ballistic transport. Actually, they are at least 1 order of magnitude lower compared to the forces in the case of elastic scattering.[17,21]

The question on whether or not the current-induced forces are conservative has been raised.[20] The current-induced forces [defined in eq 6] include the kinetic energy term, which is unable to be written as the gradient of a potential, and thus, the current-induced forces are unnecessary to be conservative. Moreover, the current-induced force field is roughly proportional to the current density. When the streamlines of current density have the tendency to rotate about a point in a vector field, the curl of the current density is nonzero, implying that the curl of the current-induced force field could be nonzero, and thus the current-induced forces are nonconservative in this case. Through molecular dynamics simulations, it has been reported that the current-induced forces may rotate the atom at the corner of a bent atomic wire.[22,23] They show that the current-induced forces are generally not conservative because the net work per revolution is nonzero. Recently, many studies have been conducted on the nonconservative nature of the current-induced forces.[24−29]

In this paper, we propose a conceptually new design of an electrically controllable single-molecule motor, propelled by the

Received: July 23, 2013
Revised: December 20, 2013
Published: January 13, 2014

   dx.doi.org/10.1021/jp4073284 | J. Phys. Chem. C 2014, 118, 2245−2252

current-induced forces due to nonequilibrium coherent electron transport. From first-principles approaches we calculate the torque that is exerted by the current-induced forces in an asymmetric single-molecule junction. The single-molecule junction consists of an asymmetric benzene molecule directly connected to platinum electrodes, as shown in Figure 1.

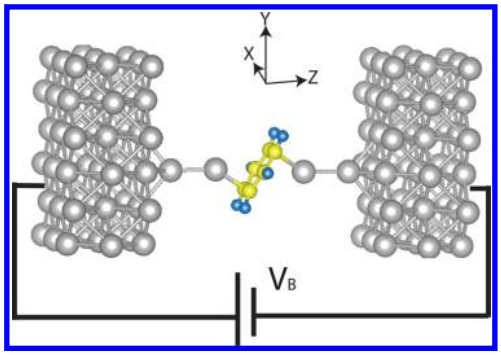

Figure 1. Schematic diagram of the Pt/benzene junction being investigated. The optimized geometry of the junction is relaxed using the VASP code. Gray, yellow, and blue balls represent Pt, carbon, and hydrogen atoms, respectively. The Pt−benzene−Pt nanostructure, where the benzene molecule is tilted, is formed through the chemical bonds between the Pt and carbon atoms. This Pt−benzene−Pt nanostructure is connected to the Pt electrodes via the Pt−Pt metallic bonding. An external bias $V_B = (E_{FR} - E_{FL})/e$ is considered to generate net torque on the benzene molecule by the current-induced forces.

Kiguchi et al. have experimentally and theoretically investigated the inelastic electron tunneling spectroscopy (IETS) and shot noise of this system, while they also measured a large conductance.[30] Such a system provides a more realistic example in demonstrating the possible rotational motion exerted by the current-induced forces at the molecular level. This molecular junction not only offers an experimentally practical system for an electrically controllable single-molecule motor but also has fundamental interest in exploring the response of forces on a single molecule due to details of the uneven electric current flow caused by the asymmetric geometry.

First, the structure of the single-molecule junction is relaxed using the Vienna Ab Initio Simulation Package (VASP). The tilted benzene molecule is roughly pivoted along the axis connecting two Pt electrodes. We observe that the relaxed configuration of the Pt/benzene junction loses mirror symmetry. The benzene ring is tilted at an angle and located slightly above the line connecting the Pt atoms. Second, we calculate the torque exerted by current-induced forces on the molecule in the relaxed geometry using the steady-current wave functions obtained self-consistently in the framework of density functional theory (DFT) in scattering approaches. To give an insight into the physical picture of the net torque exerted by the current-induced forces, we visualize the current density and the curl of current density [see Figure 2(b) and (c)]. We observe that the highly tilted benzene molecule causes the streamline flow of the current to curve considerably to one side of the benzene ring. The large current density is due to the shorter distances between the Pt atoms and the carbon atoms in the lower part of the benzene ring. The imbalanced current density results in a nonzero curl of the current density. The curl of the current density ($\vec{J} = ne\vec{v}$ in classical limit) turns the direction of the velocity of the electron and thus creates a change of the angular momentum in a unit time. Consequently, this generates uneven current-induced rotational forces which induce a net torque rotating the molecule, much like the way a stream of water rotates a waterwheel. We also observe that the net torque increases as the bias increases. Thus, the Pt/benzene junction may serve as an atomic-sized motor, which is the extreme limit of mechanical device miniaturization. To demonstrate that transverse forces can be induced by the asymmetric geometry of the molecule, we further introduce a simple physical model based on Landauer−Büttiker formalism in the tight-binding approach.[9]

The remainder of the paper is organized as follows. In section II(a), we briefly describe the theory behind the calculations for the current-induced forces in the Pt/benzene single-molecule junction based upon the DFT framework and scattering approaches. In section II(b), we introduce a simple physical model for the benzene ring that demonstrates the mechanism behind its rotation. This is done using the Landauer−Büttiker formalism in the tight-binding approach. In section III, we discuss our results, while we conclude in section IV.

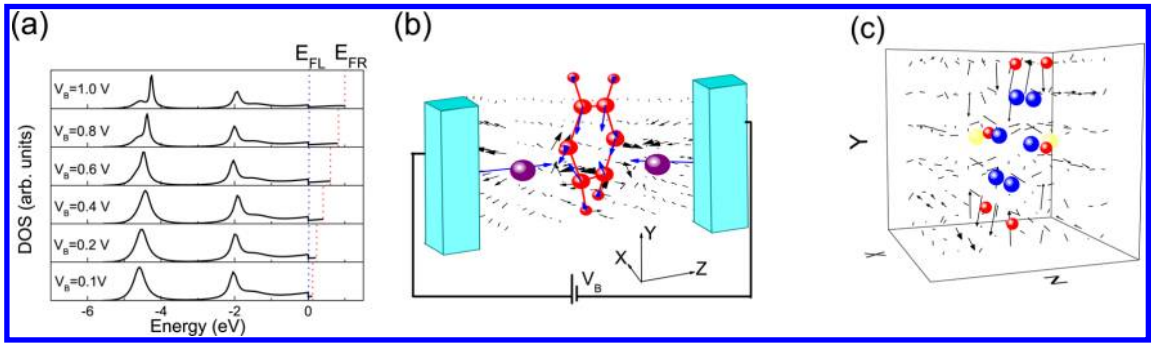

Figure 2. (a) Density of states due to the populated current-carrying states for various source−drain biases (V_B = 0.1, 0.2, 0.4, 0.6, 0.8, and 1.0 V) in the Pt/benzene junction. The left Fermi level E_{FL} (blue dotted lines) is set to be the zero of energy. The right Fermi level E_{FR} (red dotted line) refers to $V_B = (E_{FR} - E_{FL})/e$. (b) A schematic diagram of the Pt−benzene−Pt nanostructure bridging two bulk Pt electrodes modeled as electron jellium with $r_s \approx 3$. The separation of two Pt−jellium surfaces is fixed at around 9.6 au. The current-induced forces on each atom of the Pt−benzene−Pt nanostructure are shown by the 3D vector plot with blue arrows with V_B = 0.1 V. Correspondingly, the current density is represented by the 3D vector plot with black arrows. The 3D vector plot for the current density is plotted in log scale to facilitate the visualization of the smaller current density because the magnitude of the current density varies in orders of magnitude. (c) Schematic of the curl of the current density corresponding to the current density in (b). Balls represent the atoms.

dx.doi.org/10.1021/jp4073284 | J. Phys. Chem. C 2014, 118, 2245−2252

II. THEORY AND CALCULATIONS

The calculations considering the forces that are applied on the benzene molecule induced by the steady-state current follow the theory developed by Di Ventra, Pantelides, and Lang.[31,32] It is well-known that the Hellmann−Feynman theory is the key ingredient of the quantum mechanical treatment of forces acting on nuclei in molecules and solids. The Hellmann−Feynman theory is widely applied for structure optimization in material physics and chemistry. In such calculations, electrons in the electron system are in their instantaneous ground states. However, the conventional Hellmann−Feynman theory fails to apply to molecules and solids in time-dependent external fields and in transport in nanostructures and molecules. So, Di Ventra and Pantelides rigorously derived a general form of the Hellmann−Feynman-like theory considering a fully dynamical description of the many-body problem comprising electrons and ions in the classical limit of ionic motion.[26,31,33,34] According to the above theory, the Pulay terms that appear in Hellmann−Feynman theory vanish in the case of steady-state current.[35]

In our analysis, the structure of the Pt−benzene−Pt single-molecule junction is relaxed using VASP, as shown in Figure 1. With the relaxed geometry of the single-molecule junction, we calculate the current-induced forces using steady-state wave functions obtained self-consistently in the framework of DFT in scattering approaches.[36,37] To describe the physical mechanism of the proposed molecular motor, we also calculate the current-induced forces using a simple physical model based on Landauer−Büttiker formalism in the tight-binding approach.[9]

II(a). Current-Induced Forces Calculated by DFT in Scattering States. The full Hamiltonian of the system is $H = H_0 + V$, where H_0 is the Hamiltonian due to the bare Pt electrodes and V is the scattering potential of the Pt−benzene−Pt nanostructure bridging the semi-infinite Pt electrodes with a planar surface. We set the distance between two jellium surfaces to be around 9.6 au. The distances between the benzene molecule and the left (right) electrode are around 4.1 and 4.1 au, respectively. First, we calculate wave functions of H_0 due to the bimetallic junction modeled as electron jellium ($r_s \approx 3$) with an applied bias [$V_B = (\mu_R - \mu_L)/e$, where $\mu_{L(R)}$ is the chemical potential deep in the left (right) electrode] maintained by the external bias V_B. The unperturbed wave functions have the form, $\Psi^{0,L(R)}_{EK}(\mathbf{r}) = (2\pi)^{-1} e^{i\mathbf{K}\cdot\mathbf{R}} \cdot u^{L(R)}_{EK}(z)$, where $u^{L(R)}_{EK}(z)$ represents the wave function of electrons incident from the left (right) electrode under a finite bias along the z-direction before inclusion of the Pt−benzene−Pt nanostructure. The unperturbed wave functions $u^{L(R)}_{EK}(z)$ are obtained by solving the coupled Schrödinger and Poisson equations under the constraint of charge neutrality of the total system iteratively until self-consistency is reached. Deep inside the electrodes ($z \to \pm\infty$), the right- and left-moving waves satisfy the scattering boundary conditions

$$u^{L}_{EK}(z) = \sqrt{\frac{m}{2\pi\hbar^2 k_L}} \times \begin{cases} e^{ik_L z} + R_L e^{-ik_L z} & z < -\infty \\ T_L e^{ik_R z} & z > \infty \end{cases} \quad (1)$$

and

$$u^{R}_{EK}(z) = \sqrt{\frac{m}{2\pi\hbar^2 k_R}} \times \begin{cases} T_R e^{-ik_L z} & z < -\infty \\ e^{-ik_R z} + R_R e^{ik_R z} & z > \infty \end{cases} \quad (2)$$

where $\mathbf{K}$ is the electron momentum in the plane parallel to the electrode surfaces, and the z-axis is along the direction of the current. The condition of energy conservation gives $\hbar^2 k_R^2/2m = E - \hbar^2\mathbf{K}^2/2m - \nu_{eff}(\infty)$ and $\hbar^2 k_L^2/2m = E - \hbar^2\mathbf{K}^2/2m - \nu_{eff}(-\infty)$, where $\nu_{eff}(z)$ is the effective potential comprising the electrostatic potential and exchange correlation energy at the level of local density approximation.[37] Note that $\nu_{eff}(\pm\infty)$ values are the bottom of the conduction band deep inside the right and left electrodes.

The electrode−nanostructure−electrode system is considered as a unified coherent quantum system. Inclusion of the Pt−benzene−Pt nanostructure is considered in the scattering approach. The current-carrying wave functions of the total system (jellium + nanostructure) in the continuum are calculated by solving the Lippmann−Schwinger equation iteratively until self-consistency is reached

$$\Psi^{L(R)}_{E\mathbf{K}}(\mathbf{r}) = \Psi^{0,L(R)}_{E\mathbf{K}}(\mathbf{r}) + \int d^3\mathbf{r}_1 \int d^3\mathbf{r}_2 G^0_E(\mathbf{r}, \mathbf{r}_1) V(\mathbf{r}_1, \mathbf{r}_2) \Psi^{L(R)}_{E\mathbf{K}}(\mathbf{r}_2) \quad (3)$$

where $\Psi^{0,L(R)}_{E\mathbf{K}}(\mathbf{r})$ stands for the effective single-particle wave functions of the entire system, corresponding to propagating electrons incident from the left (right) electrode scattered by the nanostructure. The quantity G^0_E is Green's function for the bimetallic junction. The potential $V(\mathbf{r}_1, \mathbf{r}_2)$ that electrons experience when they scatter through the nanojunction is

$$V(\mathbf{r}_1, \mathbf{r}_2) = V_{ps}(\mathbf{r}_1, \mathbf{r}_2) + \left\{ (V_{xc}[n(\mathbf{r}_1)] - V_{xc}[n_0(\mathbf{r}_1)]) + \int d\mathbf{r}_3 \frac{\delta n(\mathbf{r}_3)}{|\mathbf{r}_1, \mathbf{r}_3|} \right\} \delta(\mathbf{r}_1 - \mathbf{r}_2) \quad (4)$$

where $V_{ps}(\mathbf{r}_1, \mathbf{r}_2)$ is the pseudopotential;[38] $n_0(\mathbf{r})$ is the electron density for the pair of biased bare electrodes; $n(\mathbf{r})$ is the electron density for the total system and $\delta n(\mathbf{r})$ is their difference; and $V_{xc}[n(\mathbf{r})]$ is the exchange−correlation potential calculated at the level of local-density approximation. A basis of 3920 plane waves is chosen in the current calculations. Localized states are obtained by a direct diagonalization of the full Hamiltonian. We note that the external bias [$V_B = (\mu_R - \mu_L)/e$] is considered in the bimetallic junction with different chemical potential deep in the electrodes. When a molecule is included in the junction, the Lippmann−Schwinger equation is applied to calculate wave functions of the entire system (electrodes + molecule) until self-consistency is achieved. Thus, the high-bias case is considered and calculated at the same footing as the zero-bias case using the Lippmann−Schwinger equation. The wave functions can be applied to calculate the current density using

$$\mathbf{J}(\mathbf{r}) = \frac{e\hbar}{mi} \int dE \int d\mathbf{K}_{\parallel} I^{RR}_{EE,K_{\parallel}}(\mathbf{r}) \quad (5)$$

where $I^{RR}_{EE',\mathbf{K}_{\parallel}}(\mathbf{r}) = [\Psi^{R}_{E,\mathbf{K}_{\parallel}}(\mathbf{r})]^* \nabla \Psi^{R}_{E',\mathbf{K}_{\parallel}}(\mathbf{r}) - \nabla[\Psi^{R}_{E,\mathbf{K}_{\parallel}}(\mathbf{r})]^* \Psi^{R}_{E',\mathbf{K}_{\parallel}}(\mathbf{r})$.

Wave functions of the continuum states and localized states are applied to calculate the current-induced forces. With the effective single-particle wave functions for transport electrons obtained in the density functional theory in the Lippmann−Schwinger equation, the Pulay-like terms vanish, and the force $\mathbf{F}$ acting on a given atom at position $\mathbf{R}$ due to the nonequilibrium current flow at finite biases is given by

dx.doi.org/10.1021/jp4073284 | J. Phys. Chem. C 2014, 118, 2245−2252

$$\mathbf{F} = -\sum_i |\psi_i\rangle \frac{\partial H}{\partial \mathbf{R}} |\psi_i\rangle - \lim_{\Delta \to 0} \int_\sigma \mathrm{d}E |\psi_\Delta\rangle \frac{\partial H}{\partial \mathbf{R}} |\psi_\Delta\rangle \tag{6}$$

where the first term on the right-hand side of eq 6 is the Hellmann−Feynman contribution to the force due to localized electronic states $|\psi_i\rangle$. The second term is the contribution to the force from the continuum states $|\psi_\Delta\rangle$. The wave functions $|\psi_\Delta\rangle$ are the eigendifferentials for each energy interval Δ in the continuum σ

$$\psi_\Delta = A \int_\Delta \mathrm{d}E \psi \tag{7}$$

where A is a normalization constant and ψ's are the effective single-particle wave functions in the continuum. In other words, eigen differentials represent wave functions in the continuum space that are square-integrable in the Hilbert space. For more details, see refs 17, 32, and 35.

II(b). Current-Induced Forces by the Tight-Binding Model. We simulate the torque that is exerted by the current-induced forces in a highly asymmetric molecular junction, i.e., a benzene ring, by introducing a simple physical model based on an analysis of a previous work using the Landauer−Büttiker formalism in the tight-binding framework.[9] The tight-binding Hamiltonian describing the benzene ring is given by the following equation

$$H = \sum_{\langle n,m \rangle} t_{nm} (c_n^\dagger c_m + c_m^\dagger c_n) \tag{8}$$

where c_n and $c_m^\dagger$ are the annihilation and creation operators, while $\langle n,m \rangle$ denotes the first nearest-neighbors and t_{nm} the hopping elements connecting the different atoms. To calculate the current-induced forces, we attach perfect square lattice leads from both the left and right sides of the benzene ring (see Figure 4(a)) with constant hopping element t. Additionally, we introduce periodic boundary conditions in the direction perpendicular to the transport (direction y) which results in a quantized wavevector k_y given by

$$k_y = \frac{2\pi q}{M} \quad (q = 1, 2, ..., M) \tag{9}$$

where q is an integer and M is the number of sites in the y-direction equal to the width of the leads. Within the tight-binding framework the bandstructure of the leads is

$$E(k_z, k_y) = 2t \cos(k_z \alpha) + 2t \cos(k_y \alpha) \tag{10}$$

which also satisfies

$$\frac{-\pi}{\alpha} \le k_z \le \frac{\pi}{\alpha} \tag{11}$$

where k_z is the wavevector defined in the transport direction and α the lattice constant of the square lattice. For electrons traveling from the left lead with some energy E, the bandstructure of eq 10 yields two energy k_z components $k_z(E, q)$ and $-k_z(E, q')$ with corresponding group velocities $v_z(q, -k_z)$ (right moving channels) and $v_z(q', k_z)$ (left moving channels) where $v_z = (1/\hbar)(\partial E(k_z, k_y)/\partial k_z)$. So, the tangential velocity defined as $v_y = (1/\hbar)(\partial E(k_z, k_y)/\partial k_y)$ corresponds to these k_z values.

Inside the benzene ring, we choose the hopping elements t_{nm} to differ randomly by a small amount of ±0.3 eV compared to the constant hopping element inside the leads (see Figure 4(a)). Also, the hopping elements that connect the leads with the benzene ring differ to the same amount under the condition that the top connection is smaller than the bottom. Furthermore, we note that roughly speaking $t_{nm} \sim 1/|r_{nm}|^s$ where r_{nm} is the distance between the sites to some power s. This kind of disorder resembles the asymmetry and the connection of the benzene molecule to the leads, introduced by first-principles calculations.

Now, consider an electron wavepacket that travels through the left lead carrying some amount of tangential momentum with a group velocity v_{in}. The electron wavepacket arrives through the lead to the scatterer, and some amount is reflected to the left with a velocity v_R, and some is transmitted to the right with a velocity v_T. So, according to the above statement, we define

$$v_{in} = \sum_q v_q(E) \tag{12}$$

and

$$v_{out} = v_R(E) + v_T(E) \tag{13}$$

where

$$v_R(E) = \sum_{q'} R_{q'}(E) v_{q'}(E) \tag{14}$$

and

$$v_T(E) = \sum_{q'} T_{q'}(E) v_{q'}(E) \tag{15}$$

$R_{q'}(E)$ and $T_{q'}(E)$ are defined as $R_{q'}(E) = \Sigma_{q'}|r_{q'q}|^2$ and $T_{q'}(E) = \Sigma_{q'}|t_{q'q}|^2$ corresponding to the reflection and transmission probabilities for an incident electron from channel q and reflected (right going) and transmitted (left going), respectively, from channel q', while the sum is over the number of open channels. According to the momentum-impulse theorem, the force per volt in a unit time (torque) that is produced is

$$F(E) = F_0(v_{in}(E) - v_{out}(E))/v_0 \tag{16}$$

where

$$F_0 = \frac{2m_e e v_0}{h}, \quad v_0 = \frac{t\alpha}{\hbar} \tag{17}$$

In our case, we choose that the constant hopping of the leads is $t = -1$ eV with lattice constant defined as $\alpha = 1$ Å, and therefore, $v_0 = 1.52 \times 10^5$ m/s and $F_0 = 6.69 \times 10^{-11}$ N/V. So, the force F_0 for 1 V is 6.69×10^{-11} N/V. Also, by symmetry the provided incoming velocity of electrons that travel through leads $v_{in} = 0$. In addition, it can be shown that if there is no asymmetry in the benzene ring the tangential force $F(E) = 0$.

By Newton's third law, the net tangential force exerted on the benzene molecule is $F_{benzene}(E) = -F(E)$, and so

$$F_{benzene}(E) = F_0(v_{out}(E) - v_{in}(E))/v_0 \tag{18}$$

III. RESULTS AND DISCUSSION

III(a). Current-Induced Forces Calculated by DFT in Scattering States. The geometry of the Pt/benzene junction is optimized by VASP shown in Figure 1, where the Pt−benzene−Pt nanostructure is formed through the chemical bonds between the Pt and carbon atoms. This Pt−benzene−Pt nanostructure is connected to the Pt electrodes via the Pt−Pt metallic bonding. The relaxed geometry shows mirror asymmetry with regard to the x−y plane. The angle between the normal of the plane where the benzene ring lies and the z-

dx.doi.org/10.1021/jp4073284 | J. Phys. Chem. C 2014, 118, 2245−2252

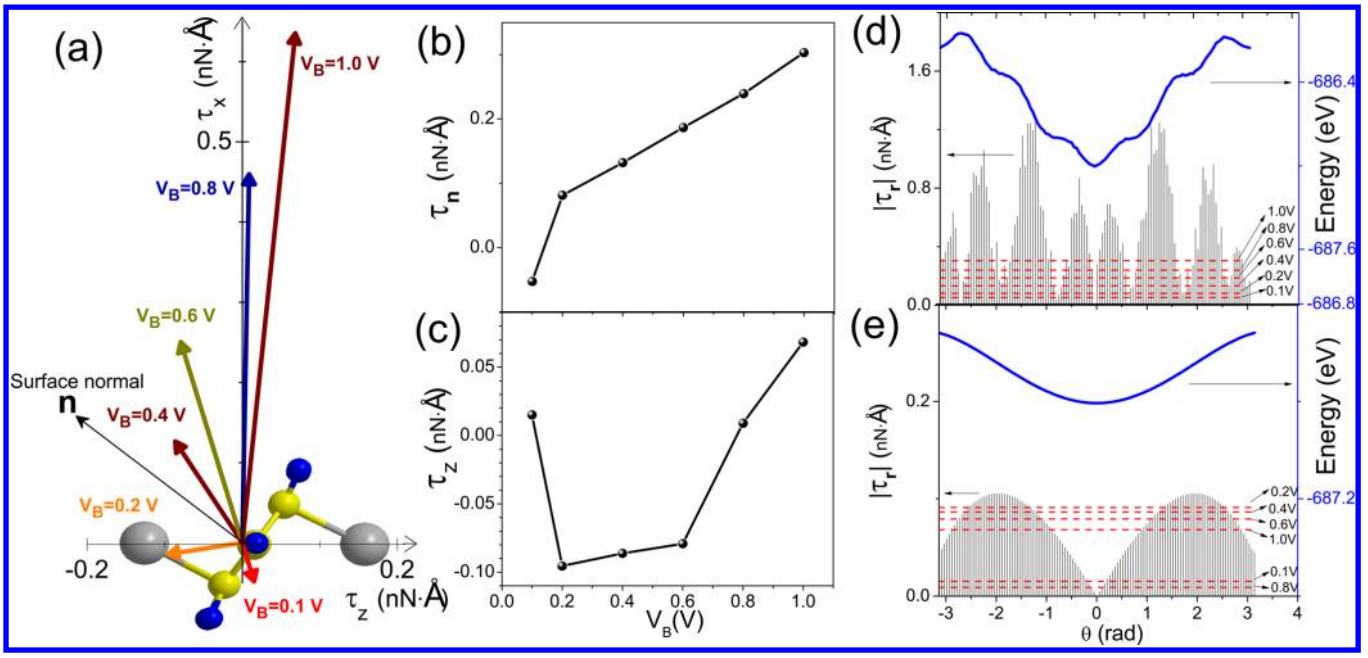

Figure 3. (a) Projection of the net torque vectors associated with the current-induced forces acting on the ions of the benzene molecule onto the x−z plane for various applied biases V_B = 0.1, 0.2, 0.4, 0.6, 0.8, and 1.0 V. The direction of the surface normal of the benzene ring is denoted as **n** (black arrow line). The horizontal (vertical) axis represents the $z(x)$ component of the torque. Electrons flow from the right to the left (negative−direction). The gray, yellow, and blue spheres represent the platinum, carbon, and hydrogen atoms of the nanostructure sandwiched between two bulk semi-infinite planar electrodes, respectively; the projection of the net torque vectors for various biases along (b) the surface normal of the benzene ring (denoted as τ_n) and (c) the z-direction (denoted as τ_z) as a function of the bias V_B. First-principles calculations of the system energy (blue solid lines) and the magnitude of the restoring torsional torque $|\tau_r|$ (black solid lines) as a function of rotation angle θ with respect to the (d) surface normal direction and (e) z-direction. The torques generated by current-induced forces at different biases (red dashed lines) are provided in both (d) and (e) for reference.

axis (the axis perpendicular to the surface of the electrodes) is 37.9°.

We model the Pt/benzene junction as the Pt−benzene−Pt nanostructure bridging two bulk Pt electrodes modeled as electron jelliums with $r_s \approx 3$. Figure 2(a) shows a series of density of states (DOSs) due to the populated current-carrying states for various source−drain biases in the Pt/benzene junction. We observe two major peaks in DOSs in all cases, where the leftside peak tends to shrink in the width and moves toward the right as the biases increase. Figure 2(b) visualizes the three-dimensional current density and compares the electron current streamline flow with the current-induced forces in the Pt/benzene junction. It is interesting to note that the center of mass of the benzene ring is located *above* the line connecting the two platinum atoms. The directions (lengths) of the blue arrows indicate the directions (magnitudes) of the current-induced forces on atoms of the Pt−benzene−Pt nanostructure for V_B = 0.1 V. The black arrows in vector field plots represent the electron current streamline flow. We observe that the benzene is subject to compressional forces in both the horizontal and vertical directions. This feature is consistent with the current-induced forces for the conventional Au/benzene junction, where the benzene molecule lies on the same plane with both electrodes and exhibits mirror symmetry.[31] More noteworthy is that the current-induced forces are highly relevant to the details of the current density. The current-induced forces acting on the ions are mostly directed along the lines tangent to the paths of the curved current streamline flows on the ions. This is particularly important in the Pt/benzene junction because of its highly asymmetric configuration, in which the streamlines of current density have the tendency to rotate around the lower part of the benzene ring due to the shorter distance between the lower part of the benzene molecule and the Pt atoms. Consequently, the curved streamlines of current density exert a net torque on the benzene molecule. Moreover, the current-induced force field is roughly proportional to the current density vector field. Figure 2(c) shows the curl of the current density. The noise of the curl of current density may be due to the fact that the current is represented in plane waves. The current-induced forces are roughly proportional to the current density. In classical sense, $\nabla \times \mathbf{J}$ is proportional to the torque τ that is $\tau \approx (\nabla \times \mathbf{J}) \cdot I/(2 \cdot m_e)$, where I is the moment of inertia. So, the fact that the curl of the current density is nonzero implies that net torque is exerted to rotate the molecule, and thus the current-induced forces are nonconservative in this sense.

Subsequently, we investigate the net torques due to the current-induced forces through the center of the benzene ring as a function of applied biases. We note that the surface normal of the benzene ring approximately lies in the x−z plane. The net torque could cause two ways of rotation about its easy axes: (1) the benzene molecule rotates about the surface normal (denoted by **n**) through the center of the benzene ring and (2) the Pt−benzene−Pt nanostructure rotates about the z-axis connecting two Pt atoms. To understand how the current-induced forces drive the rotational motion, we calculate the projections of the torque vectors along **n** and along the z-axis. Figure 3(a) shows the projections of the net torque vectors onto the x−z plane for various applied voltages. The magnitudes of the torque vectors increase, and their directions slightly change as the biases increase. The magnitudes and the directions of the torques are relevant to the detailed electronic

dx.doi.org/10.1021/jp4073284 | J. Phys. Chem. C 2014, 118, 2245−2252

structures. It is observed that the magnitudes of the projected torque vectors increase as the biases increase, and the direction of τ_n at $V_B = 0.1$ V is opposite to the directions of the projected net torques for the other five biases. As observed by Yang et al., the current-induced forces on atoms may be along or against the direction of the current flow.[19] This may explain why the net torque direction at $V_B = 0.1$ V is different from the net torque directions caused by other biases.

Figures 3(b) and 3(c) show the projection of the net torques along the surface normal of the benzene ring (denoted by τ_n) and the projection of the net torques along the z-axis (denoted by τ_z), respectively. The components of the torque vectors τ_n and τ_z tend to rotate the benzene ring about the surface normal and rotate the Pt−benzene−Pt nanostructure along the direction of the current, respectively. Although the magnitudes of the net torque along the z-axis are typically smaller than those along the surface normal of the benzene ring, we conjecture that it could be easier for the benzene molecule to rotate about the z-axis than about the surface normal of the benzene ring. The reason is that the connections between the Pt−benzene−Pt nanostructure with the Pt electrodes are metallic bonds whose bond angles are easy to change. This is in sharp contrast to the chemical bond between the carbon atom and Pt, which is directional and harder to rotate.

To further verify this conjecture, we perform total energy calculations using VASP. The total energies allow us to estimate restoring torsional torques, $\tau_r = -dE/d\theta$, that bring the Pt/benzene junction as a tortional spring back toward its equilibrium position shown in Figure 1. We rotate the benzene ring about **n** and the Pt−benzene−Pt nanostructure about the z-axis, respectively, and calculate the total energy (blue lines) using VASP as a function of the angle of rotation θ for these two cases, as shown in Figures 3(d) and 3(e). Subsequently, we calculate the magnitude of restoring torsional torques τ_r from the total energies in terms of rotation angles θ with respect to the direction of the surface normal [Figure 3(d)] and the z-direction [Figure 3(e)]. In the bar charts in Figures 3(d) and 3(e), the lengths of the bars represent the magnitudes of restoring torsional torques. In the same graphs, we also show the magnitudes of the projected net torques τ_n and τ_z represented as red horizontal dashed lines for various applied voltages. We see that rotating the Pt−benzene−Pt nanostructure about the z-axis is easier than rotating the benzene molecule about the surface normal of the benzene ring. This confirms our previous conjecture; that is, the z-axis is an easy axis to rotate. Particularly, the net torque at $V_B = 0.2$ V is large enough to rotate the Pt−benzene−Pt nanostructure by an angle of 1.2 radians, as shown in Figure 3(e). When the external voltage is turned off, the Pt/benzene junction is expected to return to the relaxed structure. Thus, the Pt/benzene junction could serve as a rotary to propel a single molecule in a controlled manner, while it also serves as a promising candidate for a single-molecule rotary machine.

III(b). Current-Induced Forces by a Tight-Binding Model. In Figure 5(a), we plot the tangential force $F_{benzene}(N/V)$ as a function of the energy E (eV) that is exerted on the benzene molecule (see Figure 4(a)), keeping in mind that always $v_{in} = 0$. In the energy region $E = [-4,-1]$ eV not shown in Figure 5(a), $F_{benzene}(E) = 0$ since the only provided open channel that is associated with the transverse velocity component is zero. For the energy region $E = [-1, 0]$ eV, there is double degeneracy and two more channels open, and as a consequence, the force becomes finite. More

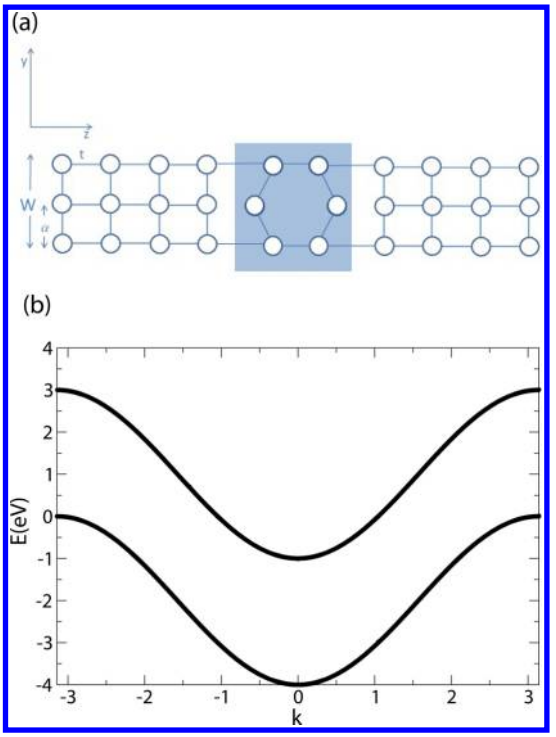

Figure 4. (a) Disordered benzene molecule (shaded area) attached to perfect square leads with periodic boundary conditions in the y direction and width of $W = 2\alpha$, where α is the lattice constant in the square leads. Disorder in the benzene molecule exists as random hopping elements t_{nm} with values that differ by an amount of ±0.3 eV compared to the constant hopping element t inside the square leads. This kind of disorder simulates the asymmetry inside the benzene ring. Also, the same amount of disorder is introduced for the connections between the benzene molecule and the leads, with the top connection smaller than the bottom. (b) Band structure calculated for the square lattice leads with periodic boundary conditions in the y-direction, constant hopping element $t = -1$ eV, and lattice constant $\alpha = 1$ Å.

specifically, these two new channels, where each one is associated with a transverse velocity component $v_{q'}$, are finite, equal, and opposite in sign, while as mentioned above the third one is zero. Also, we note that the introduction of the asymmetry through the model of disorder for the benzene ring implies unequal transmission and reflection probabilities for each channel q'. So, according to the above statements this leads to unequal reflection and transmission velocities v_R and v_T (see eqs 14 and 15), resulting in a finite force (see Figures 5(a)). As far as concerning the energy region $E = [0, 3]$ eV, the number of open channels is reduced to two. The channel that is associated with the zero transverse velocity is closed, and thus the abrupt change of force at $E = 0$ eV. It should be pointed out that in the energy area $E = [0-0.5]$ eV the main contribution to the force comes from the tangential reflected velocity v_R, while the contribution of the tangential transmitted velocity v_T is limited since the total transmission T is close to 0 (see Figure 5(b)). Finally, at the energy region $E = [0.5, 3]$ eV, there is a finite total reflection R and total transmission T which according to the above argumentation concerning the reflection and transmission probabilities $R_{q'}$ and $T_{q'}$ results in finite force.

IV. CONCLUSION

In conclusion, we have investigated the current-induced forces in the Pt/benzene junction from first-principles approaches. Also, we have demonstrated the same kind of forces introduced

dx.doi.org/10.1021/jp4073284 | J. Phys. Chem. C 2014, 118, 2245−2252

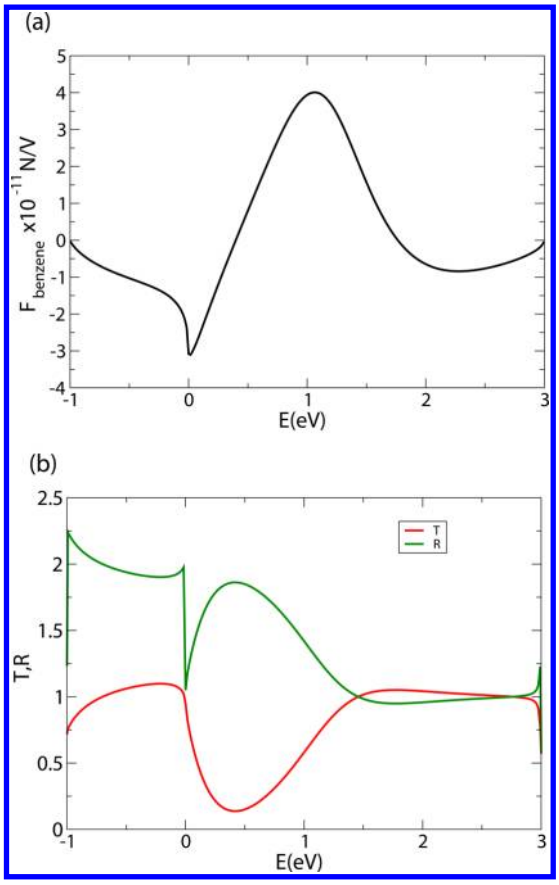

Figure 5. (a) Tangential force $F_{benzene}(N/V)$ that is exerted on the benzene molecule as a function of energy E (eV). At the beginning ($E \geq -4$ eV), not shown here, the value of force is zero since the only open channel does not contribute and force starts to take a finite value when there is a significant number of open channels; i.e., at $E = -1$ eV there are three open channels. Also, there is an abrupt change of the force at $E = 0$ eV since the number of open channels is reduced; i.e., there are only 2 open channels. (b) The total transmission T (red) and the total reflection R (green) as a function of the energy E (eV) where our system consists of perfect square lattice leads with periodic boundary conditions in the y-direction and the asymmetric benzene ring as a scatterer (see Figure 4(a)).

for a benzene molecule in a simple physical model based on the Landauer–Buttiker formula under the tight-binding framework. By first-principles calculations, we show that the current-induced forces are highly relevant to the details of the current density, especially in highly asymmetric molecular junctions. The asymmetric current streamline flows due to the tilted molecule may exert a net torque, which tends to rotate the molecule, in a manner similar to how a stream of water rotates a waterwheel. By modulating the external voltage, the magnitude and direction of the net torque exerted by the current-induced forces are controllable. We have also compared the torques exerted by the current-induced forces with the torsional restoring torques along the direction of the surface normal and the z-axis, respectively. The comparison shows that the Pt/benzene molecule is easier to rotate about the z-axis. The Pt/benzene single-molecule junction offers an experimentally practical system to explore electrically controllable single-molecule rotary motors driven by the nonequilibrium electron coherent transport. Moreover, we also demonstrate that the current-induced forces are not conservative because the curl of the current-induced force field is nonzero.

AUTHOR INFORMATION

Corresponding Author

*E-mail: yuchangchen@mail.nctu.edu.tw. Phone: +886(03) 513-1203. Fax: +886(03)572-5230.

Notes

The authors declare no competing financial interest.

ACKNOWLEDGMENTS

The authors acknowledge the support of the National Science Council (Taiwan) under Grant NSC 100-2112-M-009-012-MY3, the Ministry of Education through the Aiming for Top University Plan (MOE ATU), and the National Center for Theoretical Sciences. We also thank National Center for High-performance Computing for computing time and facilities.

REFERENCES

(1) Browne, W. R.; Feringa, B. L. Making Molecular Machines Work. *Nat. Nanotechnol.* **2006**, *1*, 25–35.
(2) Tao, C.; Cullen, W. G.; Williams, E. D. Visualizing the Electron Scattering Force in Nanostructures. *Science* **2010**, *328*, 736–740.
(3) Kudernac, T.; Ruangsupapichat, N.; Parschau, M.; Maciá, B.; Katsonis, N.; Harutyunyan, S. R.; Ernst, K.-H.; Feringa, B. L. Electrically Driven Directional Motion of a Four-Wheeled Molecule on a Metal Surface. *Nature* **2011**, *479*, 208–211.
(4) Koumura, N.; Zijlstra, R. W. J.; van Delden, R. A.; Harada, N.; Feringa, B. L. Light-Driven Monodirectional Molecular Rotor. *Nature* **1999**, *401*, 152–155.
(5) Fennimore, A. M.; Yuzvinsky, T. D.; Han, W.-Q.; Fuhrer, M. S.; Cumings, J.; Zettl, A. Rotational actuators based on carbon nanotubes. *Nature* **2003**, *424*, 408.
(6) Van Delden, R. A.; Ter Wiel, M. K. J.; Pollard, M. M.; Vicario, J.; Koumura, N.; Feringa, B. L. Unidirectional Molecular Motor on a Gold Surface. *Nature* **2005**, *437*, 1337–1340.
(7) Kay, E. R.; Leigh, D. A.; Zerbetto, F. Synthetic Molecular Motors and Mechanical Machines. *Angew. Chem., Int. Ed.* **2007**, *46*, 72–191.
(8) Gao, L.; Liu, Q.; Zhang, Y. Y.; Jiang, N.; Zhang, H. G.; Cheng, Z. H.; Qiu, W. F.; Du, S. X.; Liu, Y. Q.; Hofer, W. A.; et al. Constructing an Array of Anchored Single-Molecule Rotors on Gold Surfaces. *Phys. Rev. Lett.* **2008**, *101*, 197209.
(9) Bailey, S. W. D.; Amanatidis, I.; Lambert, C. J. Carbon Nanotube Electron Windmills: A Novel Design for Nanomotors. *Phys. Rev. Lett.* **2008**, *100*, 256802.
(10) Baber, A. E.; Tierney, H. L.; Sykes, E. C. H. A Quantitative Single-Molecule Study of Thioether Molecular Rotors. *ACS Nano* **2008**, *2*, 2385–2391.
(11) Jorn, I. R.; Seideman, T. Competition between Current-Induced Excitation and Bath-Induced Decoherence in Molecular Junctions. *J. Chem. Phys.* **2009**, *131*, 244114.
(12) Seldenthuis, J. S.; Prins, F.; Thijssen, J. M.; Van der Zant, H. S. J. An All-Electric Single-Molecule Motor. *ACS Nano* **2010**, *4*, 6681–6686.
(13) Jorn, I. R.; Seideman, T. Implications and Applications of Current-Induced Dynamics in Molecular Junctions. *Acc. Chem. Res.* **2010**, *43*, 1186–1194.
(14) Pshenichnyuk, I. A.; Cizek, M. Motor Effect in Electron Transport Through a Molecular Junction with Torsional Vibrations. *Phys. Rev. B* **2011**, *83*, 165446.
(15) Kral, P.; Seideman, T. Current-Induced Rotation of Helical Molecular Wires. *J. Chem. Phys.* **2005**, *123*, 184702; *Nat. Nanotechnol.* **2011**, *6*, 610–611.
(16) De Feyter, S. Molecular Motors: Powered by Electrons. *Nat. Nanotechnol.* **2011**, *6*, 610–611.
(17) Di Ventra, M. *Electrical Transport in Nanoscale Systems*, 1st ed.; Cambridge University Press: Cambridge, 2008.
(18) For a review see, e.g.: Sorbello, R. S. In *Solid State Physics*; Ehrenreich, H., Spaepen, F., Eds.; Academic Press: New York, 1998; Vol. *51*, p 159 and references therein.

(19) Yang, Z.; Chshiev, M.; Zwolak, M.; Chen, Y. C.; Di Ventra, M. Role of Heating and Current-Induced Forces in the Stability of Atomic Wires. *Phys. Rev. B* **2005**, *71*, 041402(R).
(20) Di Ventra, M.; Chen, Y. C.; Todorov, T. N. Are Current-Induced Forces Conservative? *Phys. Rev. Lett.* **2004**, *92*, 176803.
(21) Yang, Z.; Di Ventra, M. Nonlinear Current-Induced Forces in Si Atomic Wires. *Phys. Rev. B* **2003**, *67*, 161311(R).
(22) Brandbyge, M. Computational Nanoscience: Atomic Waterwheels Go To Work. *Nat. Nanotechnol.* **2009**, *4*, 81−82.
(23) Dundas, D.; McEniry, E. J.; Todorov, T. N. Current-Driven Atomic Waterwheels. *Nat. Nanotechnol.* **2009**, *4*, 99−102.
(24) Lu, J. T.; Brandbyge, M.; Hedegard, P. Blowing the Fuse: Berry's Phase and Runaway Vibrations in Molecular Conductors. *Nano Lett.* **2010**, *10*, 1657−1663.
(25) Todorov, T. N.; Dundas, D.; McEniry, E. J. Nonconservative Generalized Current-Induced forces. *Phys. Rev. B* **2010**, *81*, 075416.
(26) Todorov, T. N.; Dundas, D.; Paxton, A. T.; Horsfield, A. P. Nonconservative Current-Induced Forces: A Physical Interpretation. *Beilstein J. Nanotechnol.* **2011**, *2*, 727−733.
(27) Lu, J. T.; Gunst, T.; Hedegard, P.; Brandbyge, M. Current-Induced Dynamics in Carbon Atomic Contacts. *Beilstein J. Nanotechnol.* **2011**, *2*, 814−823.
(28) Bode, N.; Kusminskiy, S. V.; Egger, R.; von Oppen, F. Scattering Theory of Current-Induced Forces in Mesoscopic Systems. *Phys. Rev. Lett.* **2011**, *107*, 036804.
(29) Bode, N.; Kusminskiy, S. V.; Egger, R.; von Oppen, F. Current-Induced Forces in Mesoscopic Systems: A Scattering−matrix Approach. *Beilstein J. Nanotechnol.* **2012**, *3*, 144−162.
(30) Kiguchi, M.; Tal, O.; Wohlthat, S.; Pauly, F.; Krieger, M.; Djukic, D.; Cuevas, J. C.; Van Ruitenbeek, J. M. Highly Conductive Molecular Junctions Based on Direct Binding of Benzene to Platinum Electrodes. *Phys. Rev. Lett.* **2008**, *101*, 046801.
(31) Di Ventra, M.; Pantelides, S. T.; Lang, N. D. First-Principles Calculation of Transport Properties of a Molecular Device. *Phys. Rev. Lett.* **2000**, *84*, 979−982.
(32) Di Ventra, M.; Pantelides, S. T.; Lang, N. D. Current-Induced Forces in Molecular Wires. *Phys. Rev. Lett.* **2002**, *88*, 046801.
(33) Todorov, T. N. Tight-Binding Simulation of Current-Carrying Nanostructures. *J. Phys.: Condens. Matter* **2002**, *14*, 3049.
(34) Todorov, T. N. Time-Dependent Tight Binding. *J. Phys.: Condens. Matter* **2001**, *13*, 10125.
(35) Di Ventra, M.; Pantelides, S. T. Hellmann−Feynman Theorem and the Definition of Forces in Quantum Time-Dependent and Transport Problems. *Phys. Rev. B* **2000**, *61*, 16207.
(36) Di Ventra, M.; Lang, N. D. Transport in Nanoscale Conductors from First Principles. *Phys. Rev. B* **2001**, *65*, 045402.
(37) Lang, N. D. Resistance of Atomic Wires. *Phys. Rev. B* **1995**, *52*, 5335−5342.
(38) Bachelet, G. B.; Hamann, D. R.; Schlüter, M. Pseudopotentials that Work: From H to Pu. *Phys. Rev. B* **1982**, *26*, 4199−4228.